Journal of Colloid and Interface Science 394 (2013) 485–489

Contents lists available at SciVerse ScienceDirect

Journal of Colloid and Interface Science

www.elsevier.com/locate/jcis

A real time in situ ATR-FTIR spectroscopic study of glyphosate desorption from goethite as induced by phosphate adsorption: Effect of surface coverage

Carolina V. Waiman [a], Marcelo J. Avena [a], Alberto E. Regazzoni [b], Graciela P. Zanini [a,*]

[a] INQUISUR, Departamento de Química, Universidad Nacional del Sur, Av. Alem 1253, B8000CPB-Bahía Blanca, Argentina
[b] Gerencia Química, Centro Atómico Constituyentes, Comisión Nacional de Energía Atómica, and Instituto de Tecnología Jorge Sábato, Universidad Nacional de General San Martín, Av. General Paz 1499, B1650KNA-San Martín, Argentina

ARTICLE INFO

Article history:
Received 26 September 2012
Accepted 27 December 2012
Available online 9 January 2013

Keywords:
Competitive adsorption
Ligand exchange
Herbicides
Oxide–water interface
Glyphosate

ABSTRACT

The desorption of glyphosate from goethite as induced by the adsorption of phosphate was investigated by attenuated total reflectance Fourier transform infrared (ATR-FTIR) spectroscopy in combination with adsorption isotherms. Desorption of glyphosate was very low in the absence of phosphate. Addition of phosphate promoted glyphosate desorption. At low initial surface coverages, added phosphate adsorbed on free surface sites, mainly, displacing a small amount of glyphosate. At high initial surface coverages, on the contrary, phosphate adsorption resulted in a significant glyphosate desorption. In the latter conditions, the ratio desorbed glyphosate to adsorbed phosphate was 0.60. The desorption process can be explained by assuming that phosphate adsorbs first forming a monodentate mononuclear complex, which rapidly evolves into a bidentate binuclear complex that displaces glyphosate.

1. Introduction

Glyphosate, N-(phosphonomethyl) glycine, is a broad spectrum herbicide used in agriculture to control a large variety of weeds [1]. As a consequence of its widespread use, this herbicide has been found in surface waters, streams, and groundwaters, giving rise to a growing interest in studying the behavior of glyphosate in soils and soil constituents [2–4].

The mobility and availability of glyphosate in the environment are strongly influenced by adsorption–desorption processes on minerals [5–9], particularly on hydrous ferric oxides, which bear high affinity for glyphosate, and are ubiquitous in soils and sediments [10–12]. Goethite (α-FeOOH) is a common Fe mineral and is a very important glyphosate adsorbent. Batch experiments show that adsorption occurs in a wide pH range, decreasing monotonously from pH 3.5 to pH 9.2 [13,14]. Adsorption takes place by a ligand exchange process, resulting in the formation of inner-sphere surface complexes, in which the phosphonate group of glyphosate binds surface Fe ions displacing coordinated water molecules and/or hydroxyl ions. Spectroscopic studies by attenuated total reflectance Fourier transform infrared spectroscopy (ATR-FTIR) and X-ray photoelectron spectroscopy (XPS) indicate that monodentate mononuclear inner-sphere surface complexes are mainly formed [10,14]. Formation of such surface complexes was also accounted for using molecular orbital/density functional theory (MO/DFT) [15].

In natural environments, glyphosate adsorption on mineral surfaces is affected by the presence of other substances, such as other pesticides, ions, organic matter, fertilizers, and surfactants. It is well known that phosphate has a strong effect on glyphosate adsorption [16–19]. Phosphate is a macronutrient for plants, and it is frequently applied to soils as a fertilizer [20]. As it occurs with glyphosate, phosphate adsorbs on goethite, as well as on other mineral surfaces, by a ligand exchange process forming inner-sphere complexes [21–24]. Thus, competition of phosphate and glyphosate for the adsorption sites of goethite may play an important role in determining the bioavailability, degradation, and fate of glyphosate in nature [17,25–29].

Competitive adsorption between glyphosate and phosphate was studied so far by batch adsorption–desorption experiments. Gimsing and Borggaard [6,28,30] induced glyphosate desorption from goethite by adding phosphate and *vice versa*. They showed that phosphate inhibits glyphosate adsorption and under certain conditions is able to desorb glyphosate completely [31–33].

In spite of these important data, there is no information in the literature referring to the mechanism of the competition process. For instance, it is unclear whether phosphate displaces adsorbed glyphosate directly or phosphate adsorption onto unoccupied surface sites takes place prior attacking the bonds that link the phosphonate moiety to the surface. Inspection of the evolution of the surface complexes involved in this reaction by ATR-FTIR could give valuable information in this respect. With this aim, the present article reports an ATR-FTIR study of glyphosate desorption from goethite as induced by the presence of phosphate.

* Corresponding author. Fax: +54 291 4595160.
E-mail address: gzanini@uns.edu.ar (G.P. Zanini).

0021-9797/$ - see front matter © 2013 Elsevier Inc. All rights reserved.
http://dx.doi.org/10.1016/j.jcis.2012.12.063

2. Experimental section

2.1. Goethite synthesis and characterization

Goethite particles were synthesized as described by Puccia et al. [34], following the methodology proposed by Atkinson et al. [35]. Briefly, a 5 M NaOH solution was added dropwise (10 mL min^{-1}) to a 0.1 M $Fe(NO_3)_3{\cdot}9H_2O$ aqueous solution until the pH was 12; this was done under a CO_2-free atmosphere. The resulting suspension was aged at 60 °C for 3 days. The precipitate was then washed with water until the conductivity of the supernatant was lower than 10 μS cm^{-1}. The so-prepared goethite was stored as a stock suspension at pH 5.

The XRD pattern of the synthesized solid was typical of goethite. Its N_2-BET surface area was 68.9 m^2 g^{-1}.

2.2. Adsorption isotherms

Glyphosate and phosphate adsorption isotherms were obtained by batch equilibration experiments. They were performed by adding 0.2 mL of the stock goethite suspension (22.10 g L^{-1}) to 15 mL polypropylene centrifuge tubes, to which 9.8 mL of an aqueous solution of known concentration of either glyphosate or phosphate was added; the concentration of the background electrolyte (KCl) was 0.1 M. The pH of these dispersions was adjusted to 4.5 and kept constant by adding a few microliters of either KOH or HCl solutions. The tubes were shaken overnight with an end-over-end rotator, and then, the supernatants separated by centrifugation. The concentration of glyphosate in the supernatants was measured by the UV–Vis spectrophotometric method proposed by Waiman et al. [36]. The concentration of phosphate was quantified by the molybdenum blue method proposed by Murphy and Riley [37]. UV–Vis spectra were recorded with an Agilent 8453 UV–Vis diode array spectrophotometer equipped with a 1 cm Hellma quartz cell.

The amount of glyphosate and phosphate adsorbed by goethite (surface excess value, Γ_G and Γ_P, respectively) was calculated solving the mass balance of the systems.

2.3. ATR-FTIR spectroscopy

ATR-FTIR spectra were obtained using a Nicolet Nexus 470 FTIR spectrometer equipped with a DTGS detector, a SMART-ARK ATR accessory and a ZnSe crystal (area: 10 × 72 mm, incident angle: 45°, total reflections: 12). Experiments were performed as follows: 200 μL of a 10 g L^{-1} goethite dispersion equilibrated at pH 4.5 was placed on the ZnSe crystal and evaporated to dryness at room temperature [34]. Then, the film was covered with 2 mL of a 0.1 M KCl solution (pH 4.5), and a blank spectrum recorded. The electrolyte solution was withdrawn, and a fresh 0.1 M KCl solution (pH 4.5) containing glyphosate at a desired concentration was added. Spectra were then recorded as a function of time. After equilibration, the supernatant was replaced by a fresh aliquot of the same glyphosate solution, and the spectra were recorded again. This was repeated until no spectral variations were detected. This procedure ensures that the concentration of glyphosate in equilibrium with the goethite film is that of the starting solution. Afterward, the desorption run was started by replacing the glyphosate solution with a 100 μM phosphate solution (0.1 M KCl; pH 4.5), and the spectra recorded as a function of time.

Additional ATR-FTIR experiments were performed as described above to register the spectra of adsorbed phosphate as a function of phosphate concentration.

In all cases, each recorded spectrum was the average of 256 scans, with a spectral resolution of 4 cm^{-1}. The time needed to collect each spectrum was 3 min.

The working temperature was 25 ± 2 °C.

3. Results and discussion

Fig. 1 shows the adsorption isotherms of glyphosate and phosphate at pH 4.5. Both anions adsorb significantly on goethite. The results are similar to those reported by Sheals et al. [10] and Antelo et al. [22]. A data fit with the Langmuir equation ($\Gamma = \Gamma_m KC/(1+KC)$), where K and Γ_m are the Langmuir constant and the adsorption maximum, respectively, yielded the values K = 0.45 ± 0.27 μM^{-1} and Γ_m = 2.82 ± 0.03 μmol/m^2 for phosphate, and K = 0.11 ± 0.02 μM^{-1} and Γ_m = 2.34 ± 0.04 μmol/m^2 for glyphosate. Therefore, the affinity of phosphate for the goethite surface is larger than that of glyphosate. In addition, phosphate adsorption maximum is somewhat higher. This fact was already noted by Gimsing and Borggaard [30], who suggested that the different adsorption maxima might be the result of the different molecular sizes of phosphate and glyphosate.

Fig. 2 shows the ATR-FTIR spectra of adsorbed glyphosate and phosphate. In both cases, the equilibrium aqueous concentration is 100 μM, which according to the respective adsorption isotherms (Fig. 1), corresponds to surface excess values of 2.0 and 2.7 μmol m^{-2} for glyphosate and phosphate, respectively. These spectra correspond to inner-sphere surface complexes of glyphosate and phosphate, and are different to the corresponding spectra of the respective ions in solution [10,14,38]. In the case of glyphosate, IR absorption bands appear at 1400, 1329, 1143, 1013 (shoulder) and 988 cm^{-1}, and correspond to the ν_s(C—O), ν(C—O—P), ν_a(P—O) and ν(P—OFe) (antisymmetric and symmetric) vibration modes, respectively. According to Sheals et al. [10], these bands reflect the formation of monodentate mononuclear inner-sphere complexes, in which the phosphonate moiety is directly bonded to surface Fe(III) centers. Following the analysis of Sheals et al., the position of the carboxylate bands indicates no or extremely low carboxylate–surface interactions. Similar conclusions were reached by Barja et al. [14].

In the case of phosphate, IR absorption bands appear at 1123, 1095 (shoulder), 1040 (shoulder), and 1007 cm^{-1}. According to Tejedor-Tejedor and Anderson [21], they correspond to the ν(P═O), ν(P—O) (A_1), ν(P—O) (B_2) and ν_a(P—OFe) modes. There is also a shoulder at 952 cm^{-1}. Persson et al. [39] have informed a similar shoulder at 939 cm^{-1}, assigned to the P—OH vibration, and Tejedor-Tejedor and Anderson [21] informed also a weak band

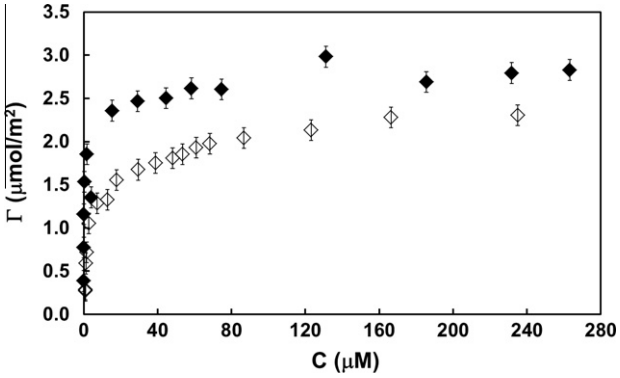

Fig. 1. Glyphosate (◇) and phosphate (♦) adsorption isotherms on goethite in 0.1 M KCl at pH 4.5. C is the equilibrium concentration of either glyphosate or phosphate. Error bars correspond to standard deviation calculated from three different isotherms.

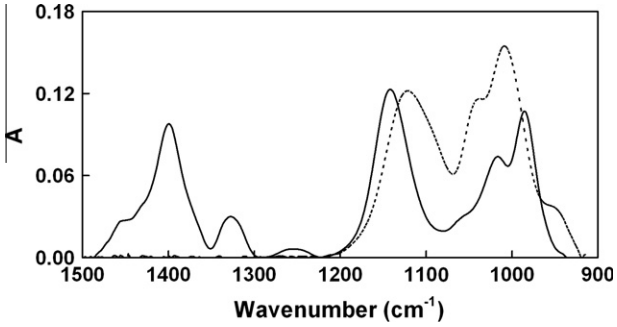

Fig. 2. ATR-FTIR spectra of adsorbed glyphosate (full line) and adsorbed phosphate (dotted line) at pH 4.5 and 0.1 M KCl. Equilibrium aqueous concentration was 100 μM in both cases.

at 982 cm^{-1}, attributed to ν_s(P—OFe) and/or ν(P—OH). Tejedor-Tejedor and Anderson [21] and Luengo et al. [23] indicate that spectra similar to those shown in Fig. 2 correspond to a mixture of the protonated and nonprotonated forms of bidentate binuclear complexes. On the contrary, Persson et al. [39] suggest a purely monodentated coordination. A recent reinterpretation of IR data together with adsorption modeling has led Rahnemaie et al. [24] to conclude that the bidentate binuclear complex prevails at high pH and low surface coverage, whereas the protonated monodentate mononuclear complex is dominant at low pH and high surface coverage. Even though there may still be controversies about the binding mode of phosphate to goethite, the general consensus is that spectra like the one shown in Fig. 2 correspond to inner-sphere surface complexes, and that both monodentate and bidentate phosphate complexes can actually be present.

Fig. 3 shows the evolution of the ATR-FTIR spectra during the desorption of glyphosate induced by the addition of phosphate. Three different cases are shown, each corresponding to a different initial glyphosate surface excess $\Gamma_{G,i}$. Fig. 3a presents the data for the lowest explored glyphosate surface excess; that is, $\Gamma_{G,i}$ = 1.1 μmol m^{-2}. Most spectral changes are observed in the 1200–900 cm^{-1} range, where bands due to adsorbed phosphate increase with time. In the range 1500–1300 cm^{-1}, on the other hand, changes are feeble; yet, a very small decrease in the carboxylate bands at 1400 and 1329 cm^{-1} is observed.

The other extreme is shown in Fig. 3c, where the initial glyphosate surface excess is 2.3 μmol m^{-2}. In this case, the whole spectrum changes gradually, and a considerable decrease in the intensity of the bands due to glyphosate and a concomitant increase in those due to phosphate are observed. As a result, an isosbestic point becomes apparent at 1124 cm^{-1}. At ca. 970 cm^{-1}, there seems to be an additional isosbestic point, but it is less clearly defined. The presence of the isosbestic points in the studied system suggests that both substances are exchanged in the same proportion during the reaction. It also suggests that the shape of the individual glyphosate and phosphate spectra is rather invariant during the reaction (only intensity varies), indicating that the presence of phosphate at the surface does not change the binding mode (or modes) of glyphosate and *vice versa*.

The intermediate case is shown in Fig. 3b, where the initial glyphosate surface excess is 1.6 μmol m^{-2}. Here, a decrease in the intensity of the bands due to glyphosate and an increase in those due to phosphate are also seen, but the changes are less marked than in Fig. 3c. In addition, the isosbestic point is less clearly defined, indicating that the anions are not exchanged at the same ratio throughout the reaction.

Desorption of glyphosate can easily be assessed from the data in Fig. 3. However, the overlap of bands in the region 1200–900 cm^{-1} precludes recording the adsorption of phosphate. To overcome this

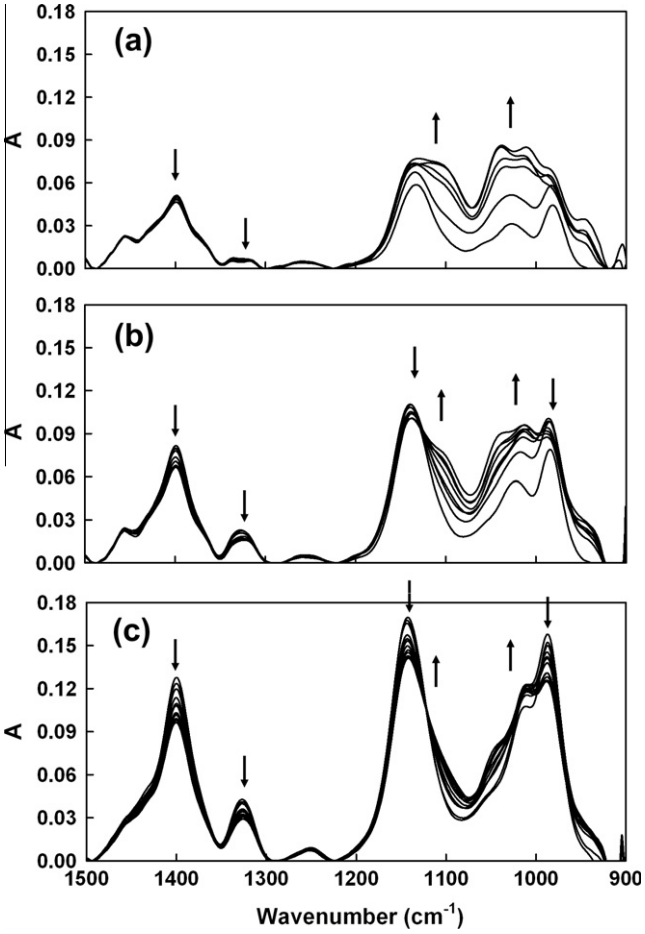

Fig. 3. ATR-FTIR glyphosate desorption experiments induced by the addition of 100 μM phosphate. Initial surface coverage with glyphosate: (a) 1.1 μmol m^{-2}, (b) 1.6 μmol m^{-2}, (c) 2.3 μmol m^{-2}. The arrows indicate the direction of evolution of the main bands during 60 min of reaction. Following the directions given by the arrows, the spectra correspond to the following times after phosphate addition: (a) 0 min, 1.5 min, 11.5 min, 22.5 min, 33.5 min, 55 min; (b) 0 min, 1.5 min, 4.5 min, 7.5 min, 18.5 min, 29.5 min, 40.5 min, 50 min, 58 min; (c) 0 min, 1.5 min, 4.5 min, 12.5 min, 18.5 min, 24.5 min, 31.5 min, 37.5 min, 41.5 min, 58 min.

difficulty, in what follows, we shall analyze the data in terms of Eqs. (1)–(4). For this purpose, we assume that the spectral features of adsorbed glyphosate are independent of each other, that they are additive, and that the absorbance of each species is proportional to the respective surface excess.

$$A = A_G + A_P \tag{1}$$

$$A = \kappa_G \Gamma_G + \kappa_P \Gamma_P \tag{2}$$

where A, A_G, and A_P are, respectively, the total absorbance, the absorbance of adsorbed glyphosate, and the absorbance of adsorbed phosphate at a given wavenumber, and κ_G and κ_P are proportionality constants. For 1400 cm^{-1}, where only glyphosate absorbs, and 1100 cm^{-1}, where phosphate absorption is important, but glyphosate absorption is relatively low (Fig. 2). Eq. (2) takes the form:

$$A^{1400} = \kappa_G^{1400} \Gamma_G \tag{3}$$

$$A^{1100} = \kappa_G^{1100} \Gamma_G + \kappa_P^{1100} \Gamma_P \tag{4}$$

where the superscripts 1400 and 1100 denote the wavenumbers. Therefore, provided κ_G^{1400}, κ_G^{1100}, and κ_P^{1100} are known, Γ_G can be calculated using Eq. (3), and Γ_P can be obtained from Eq. (4).

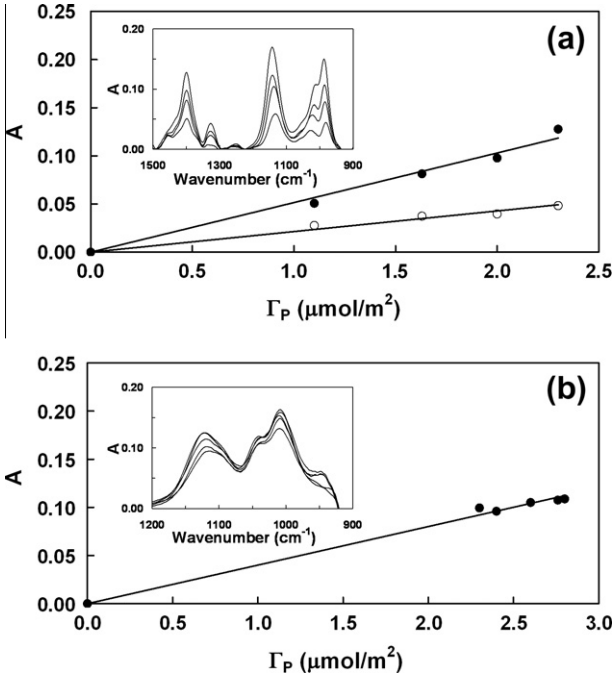

Fig. 4. Absorbance versus Γ_G or Γ_P for: (a) glyphosate at 1400 cm^{-1} (●) and at 1100 cm^{-1} (○) and (b) phosphate. The insets show the ATR-FTIR spectra of the corresponding data.

To evaluate the values of κ_G^{1400}, κ_G^{1100}, and κ_P^{1100}, spectra of goethite films equilibrated with pure glyphosate and phosphate solutions of known equilibrium concentrations were recorded. Then, A^{1400} and A^{1100} were plotted as a function of the respective Γ, the value of which was obtained from the corresponding adsorption isotherm (Fig. 1). These plots are shown in Fig. 4. Straight lines were found in all cases, and the values $\kappa_G^{1400} = 0.054 \pm 0.002$ m^2 μmol^{-1} ($R^2 = 0.984$), $\kappa_G^{1100} = 0.0167 \pm 0.0008$ m^2 μmol^{-1} ($R^2 = 0.975$) and $\kappa_P^{1100} = 0.0436 \pm 0.0007$ m^2 μmol^{-1} ($R^2 = 0.992$) were obtained from their slopes.

Despite the uncertainties of the so-derived Γ values, it is worthwhile analyzing their evolution, at least semiquantitatively. Fig. 5a, which presents the data for the lowest initial glyphosate surface excess that was studied ($\Gamma_{G,i} = 1.1$ μmol m^{-2}), shows that Γ_P increases from 0 to 1.4 μmol m^{-2}, whereas Γ_G decreases from 1.1 μmol m^{-2} to 0.9 μmol m^{-2} during the reaction. Since there is an important adsorption of phosphate and a small desorption of glyphosate, the total adsorption ($\Gamma_T = \Gamma_P + \Gamma_G$) increases monotonously as the reaction proceeds, up to 2.3 μmol m^{-2}. Fig. 5b depicts the intermediate situation ($\Gamma_{G,i} = 1.6$ μmol m^{-2}). Adsorbed phosphate increases up to 1.3 μmol m^{-2} after 60 min of reaction. Simultaneously, glyphosate decreases from 1.6 to 1.3 μmol m^{-2}. The total adsorption increases now to 2.6 μmol m^{-2}. At the higher initial glyphosate surface excess case ($\Gamma_{G,i} = 2.3$ μmol m^{-2}), the trend is more marked, and phosphate adsorption reaches 0.9 μmol m^{-2}, whereas glyphosate desorbs from 2.3 to 1.9 μmol m^{-2}. The total adsorption increases with time, reaching a value of 2.8 μmol m^{-2}.

The overall analysis of Fig. 5 indicates that the amounts of adsorbed phosphate and desorbed glyphosate depend on the initial glyphosate surface excess. At low $\Gamma_{G,i}$, high phosphate adsorption promotes a rather low glyphosate desorption. On the contrary, at high $\Gamma_{G,i}$, a relatively low phosphate adsorption promotes a relatively high glyphosate desorption. Glyphosate desorption by phosphate can be better analyzed by plotting desorbed glyphosate ($\Gamma_{G,i} - \Gamma_G$) as a function of adsorbed phosphate. This is done in Fig. 6. For the lowest $\Gamma_{G,i}$ case, phosphate adsorption takes place

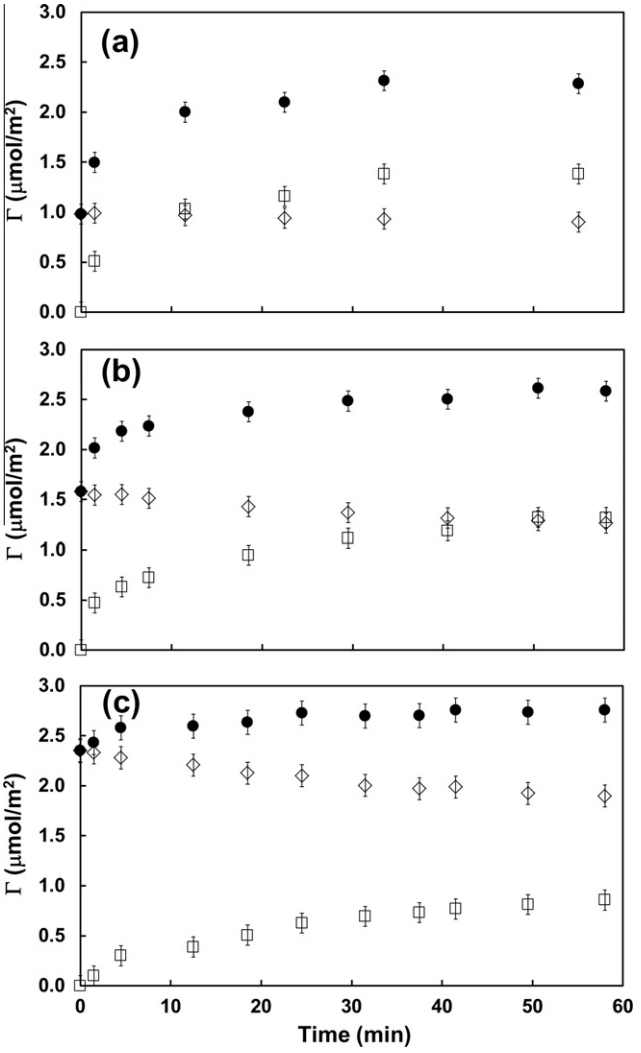

Fig. 5. Time evolution of Γ_G (◇), Γ_P (□) and Γ_T (●) during glyphosate desorption experiments after addition of 100 μM phosphate. Figures correspond to different initial surface excesses with glyphosate: (a) $\Gamma_{G,i} = 1.1$ μmol m^{-2}, (b) $\Gamma_{G,i} = 1.6$ μmol m^{-2} and (c) $\Gamma_{G,i} = 2.3$ μmol m^{-2}.

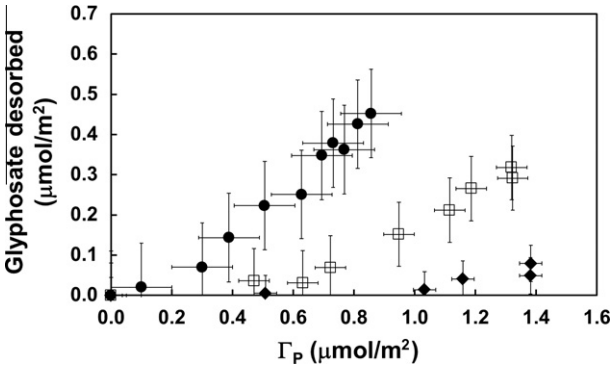

Fig. 6. Desorbed glyphosate versus adsorbed phosphate for different initial surface coverages: (●) $\Gamma_{G,i} = 2.4$ μmol m^{-2}, (□) $\Gamma_{G,i} = 1.6$ μmol m^{-2}, (♦) $\Gamma_{G,i} = 1.1$ μmol m^{-2}.

without a detectable glyphosate desorption until Γ_P is around 1.1 μmol m^{-2}. Further phosphate adsorption causes a small glyphosate desorption. The results indicate that at the beginning,

phosphate adsorbs mainly on free surface sites, and that displacement of glyphosate is detectable only when the surface becomes highly populated by both substances. For the intermediate case, glyphosate desorption becomes detectable when Γ_P is around 0.4 μmol m^{-2}. The slope of the curve, that is, the ratio desorbed glyphosate/adsorbed phosphate, increases gradually as phosphate adsorbs, also suggesting that phosphate occupies at the beginning of the reaction available free surface sites; mainly, the displacement of glyphosate becomes more effective as the overall surface coverage increases. For the highest $\Gamma_{G,i}$ case, a linear relationship between desorbed glyphosate and adsorbed phosphate is observed; the slope being 0.60 at $\Gamma_P > 0.2$ μmol m^{-2}.

These results can be rationalized in terms of the following kinetic scheme (Eqs. (5)–(8)).

$$\equiv FeOPO(OH)G + OH^- \overset{k_{dG,0}}{\rightarrow} \equiv FeOH + OPO(OH)G^- \quad (5)$$

$$\equiv FeOH + H_2PO_4^- \overset{k_{a1,P}}{\rightarrow} \equiv FeOPO(OH)_2OH^- \quad (6)$$

$$\equiv FeOH + \equiv FeOPO(OH)_2 \overset{k_{a2,P}}{\rightarrow} (\equiv FeO)_2PO(OH)H_2O \quad (7)$$

$$\equiv FeOPO(OH)G + \equiv FeOPO(OH)_2 \overset{k_{dG,P2}}{\rightarrow} (\equiv FeO)_2PO(OH) + OP(OH)_2G \quad (8)$$

$$\equiv FeOPO(OH)G + H_2PO_4^- \overset{k_{dG,P1}}{\rightarrow} (\equiv FeOPO)(OH)_2 + OPO(OH)G^- \quad (9)$$

Note that in Eqs. (5), (8), and (9), only the phosphonate group of glyphosate is explicitly written; the rest of the molecule is denoted as G.

Eq. (5) represents glyphosate desorption prompt by ligand exchange with hydroxyl ions, Eqs. (6) and (7) depict the formation of bidentate binuclear phosphate surface complexes as a successive reaction, and Eq. (8) symbolize the attack of a monodentate phosphate surface complex on an adjacent glyphosate surface complex. Eq. (9) illustrates the attack of dissolved phosphate onto an adsorbed glyphosate species to form a monodentate surface complex. This path competes unfavorably with reaction 6, as long as free sites remain available. Thus, the distribution of surface species at any given time shall be determined by the interplay of the different rate processes. Under our experimental condition, reaction 5 is exceedingly sluggish (see Supplementary material); hence, glyphosate desorption takes place mainly through path 8, which becomes increasingly important as the product $\Gamma_G \times \Gamma_P$ increases. Once the overall surface excess reaches saturation, phosphate adsorption is arrested, because it becomes controlled by reactions 5 and 9.

4. Conclusions

Desorption of glyphosate is promoted by the addition of phosphate. When glyphosate is initially adsorbed at low surface coverages, added phosphate adsorbs mainly on free surface sites, displacing a small amount of glyphosate. At high initial glyphosate surface coverages, phosphate displaces glyphosate significantly. The finding of isosbestic points under the latter conditions indicates that the presence of phosphate at the surface does not change the binding mode (or modes) of glyphosate and *vice versa*. The results also suggest that phosphate adsorption onto unoccupied surface sites takes place prior the attack of the bonds that link glyphosate to the surface.

Acknowledgments

This work was financed by CONICET, ANPCYT and UNS. O. Pieroni is thanked for her help with IR measurements. Carolina Waiman thanks CONICET for the doctoral fellowship. M.J.A., A.E.R. and G.P.Z. are members of CONICET.

Appendix A. Supplementary material

Supplementary data associated with this article can be found, in the online version, at http://dx.doi.org/10.1016/j.jcis.2012.12.063.

References

[1] G.M. Williams, R. Kroes, I.C. Munro, Regul. Toxicol. Pharmacol. 31 (2000) 117.
[2] L. Candela, J. Álvarez-Benedí, M.T. Condesso de Melo, P.S.C. Rao, Geoderma 140 (2007) 8.
[3] R.C. Pessagno, R.M. Torres Sánchez, M. dos Santos Afonso, Environ. Pollut. 153 (2008) 53.
[4] P.J. Peruzzo, A.A. Porta, A.E. Ronco, Environ. Pollut. 156 (2008) 61.
[5] W.E. Dubbin, G. Sposito, M. Zavarin, Soil Sci. 165 (9) (2000) 699.
[6] O.K. Borggaard, A.L. Gimsing, Pest Manage. Sci. 64 (2008) 441.
[7] C.M. Jonsson, P. Persson, S. Sjöberg, J.S. Loring, Environ. Sci. Technol. 42 (2008) 2464.
[8] C.N. Albers, G.T. Banta, P.E. Hansen, O.S. Jacobsen, Environ. Pollut. 157 (2009) 2865.
[9] G.A. Khoury, T.C. Gehris, L. Tribe, R.M. Torres Sánchez, M. dos Santos Afonso, Appl. Clay Sci. 50 (2010) 167.
[10] J. Sheals, S. Sjöberg, P. Persson, Environ. Sci. Technol. 36 (2002) 3090.
[11] A.L. Gimsing, O.K. Borggaard, M.J. Bang, Soil Sci. 55 (2004) 183.
[12] P. Mäkie, G. Westin, P. Persson, L. Österlund, J. Phys. Chem. A 115 (32) (2011) 8948.
[13] J.S. McConnell, L.R. Hossner, J. Agric. Food Chem. 33 (1985) 1075.
[14] B.C. Barja, M. dos Santos Afonso, Environ. Sci. Technol. 39 (2005) 585.
[15] L. Tribe, K.D. Kwon, C.C. Trout, J.D. Kubicki, Environ. Sci. Technol. 40 (2006) 3836.
[16] P. Sprankle, W.F. Meggitt, D. Penner, Weed Sci. 23 (1975) 229.
[17] H.M. Dion, J.B. Harsh, H.H.J. Hill, Radioanal. Nucl. Chem. 249 (2001) 385.
[18] H. de Jonge, L.W. de Jonge, O.H. Jacobsen, T. Yamaguchi, P. Moldrup, Soil Sci. 166 (2001) 230.
[19] S. Bott, T. Tesfamariam, A. Kania, B. Eman, N. Aslan, V. Römheld, G. Neumann, Plant Soil 342 (1–2) (2011) 249.
[20] R. Olsson, R. Giesler, P.J. Persson, Interface Sci. 353 (2011) 263.
[21] M.I. Tejedor-Tejedor, M.A. Anderson, Langmuir 6 (3) (1990) 602.
[22] J. Antelo, M. Avena, S. Fiol, R. López, F.J. Arce, Interface Sci. 285 (2005) 476.
[23] C. Luengo, M. Brigante, J. Antelo, M.J. Avena, Interface Sci. 300 (2006) 511.
[24] R. Rahnemaie, T. Hiemstra, W.H. Van Riemsdijk, Langmuir 23 (2007) 3680.
[25] A. Piccolo, G. Celano, M. Arienzo, A.J. Mirabella, Environ. Sci. Health Part B 29 (1994) 1105.
[26] H. de Jonge, L.W. de Jonge, Chemosphere 39 (5) (1999) 753.
[27] A.L. Gimsing, O.K. Borggaard, P. Sestoft, Environ. Sci. Technol. 39 (2004) 1718.
[28] A.L. Gimsing, C. Szilas, O.K. Borggaard, Geoderma 138 (2007) 127.
[29] B. Zhao, J. Zhang, J. Gong, H. Zhang, C. Zhang, Geoderma 149 (2009) 290.
[30] A.L. Gimsing, O.K. Borggaard, Clays Clay Miner. 3 (2001) 270.
[31] A.L. Gimsing, O.K. Borggaard, Clay Miner. 37 (2002) 509.
[32] A.L. Gimsing, O.K. Borggaard, Int. J. Environ. Anal. Chem. 82 (8–9) (2002) 545.
[33] A.L. Gimsing, O.K. Borggaard, Clays Clay Miner. 55 (1) (2007) 108.
[34] V. Puccia, C. Luengo, M. Avena, Colloids Surf. A 348 (2009) 221.
[35] R.J. Atkinson, A.M. Posner, J.P. Quirk, J. Phys. Chem. 71 (1967) 550.
[36] C.V. Waiman, M.J. Avena, M. Garrido, B. Fernández Band, G.P. Zanini, Geoderma 170 (2012) 154.
[37] J. Murphy, J.P. Riley, Anal. Chim. Acta 27 (1962) 31.
[38] E.J. Elzinga, J. Colloid Interface Sci. 308 (2007) 53.
[39] P. Persson, N. Nilsson, S. Sjöberg, J. Colloid Interface Sci. 177 (1996) 263.